Cent. Eur. J. Phys. • 8(2) • 2010 • 207-220
DOI: 10.2478/s11534-009-0133-6

VERSITA

Central European Journal of **Physics**

Photothermal methods for determination of thermal properties of bulk materials and thin films

Research Article

Jerzy Bodzenta*, Anna Kaźmierczak-Bałata, Jacek Mazur

Institute of Physics, Silesian University of Technology, Gliwice, Poland

Received 8 December 2008; accepted 2 September 2009

Abstract: Information on the thermal properties of materials is very important both in fundamental physical research and in engineering applications. The development of materials with desirable heat transport properties requires methods for their experimental determination. In this paper basic concepts of the measurement of parameters describing the heat transport in solids are discussed. Attention is paid to methods utilizing non-stationary temperature fields, especially to photothermal methods in which the temperature disturbance in the investigated sample is generated through light absorption. Exemplary photothermal measuring techniques, which can be realized using common experimental equipment, are described in detail. It is shown that using these techniques it is possible to determine the thermal diffusivity of bulk transparent samples, opaque and semi-transparent plate-form samples, and the thermal conductivity of thin films deposited on thick substrates. Results of the investigation of thermal diffusivity of the ground in the polar region, which is based on the analysis of the propagation of the thermal wave generated by sun-light, are also presented. Based on chosen examples one can state that photothermal techniques can be used for determination of the thermal properties of very different materials.

PACS (2008): 65.40.-b, 66.30.Xj, 66.70.-f, 68.60.-p

Keywords: measuring methods • photothermal methods • thermal properties • thermal waves in solids

© *Versita Warsaw and Springer-Verlag Berlin Heidelberg.*

1. Introduction

The knowledge of thermal properties of materials is very important both in fundamental physical research and in engineering applications. In solid state physics investigations of the thermal conductivity give information about lattice dynamics in crystalline solids. In the case of conducting materials an analysis of the heat transport also allows us to acquire information about charge carriers and interactions between phonons and carriers systems [1]. A present-day technology demands materials of well-defined thermal conductivity. The challenge in development of material science is to produce structures with extremely high thermal conductivity for effective heat abstraction and extremely low thermal conductivity for thermal barriers. Overheating limits performance of electronic devices and lasers. The development of materials with high thermal conductivity and methods of effective cooling is therefore an important task [2]. On the other hand there are also devices in which a good thermal insulation plays a key role. For example, to avoid overheating, gas turbine blades are covered with special coatings being

*E-mail: Jerzy.Bodzenta@polsl.pl

thermal barriers [3]. The development of materials with desirable heat transport properties requires a knowledge of the mechanisms of heat transport, but also requires experimental methods for determination of thermal properties.

Several interesting possibilities for the determination of heat transport properties are possible based upon analysis of a propagation of non-stationary temperature fields in a sample, especially those which use a light for the generation of the disturbance of temperature field – *i.e.* photothermal methods. The aim of this paper is to present selected photothermal measuring methods used for determination of the thermal diffusivity or the thermal conductivity of bulk materials and thin films. The majority of methods presented in this paper apply the mirage effect for detection of the temperature disturbance. This detection technique is quite convenient in the laboratory experiments. There are also other techniques which can be use for signal detection, such as infrared radiometry - the most popular technique in industrial application, photoacoustic detection, temperature-modulated reflectance, semiconductor temperature sensors, thermocouples, *etc.* A more detailed review of experimental techniques used in photothermal measurements can be found elsewhere [4].

The next section is devoted to general characterization of experimental techniques used for determination of parameters describing the heat transport in solids, *i.e.* the thermal conductivity and the thermal diffusivity. Special attention is paid to methods based on non-stationary heat fluxes and among them, to the methods utilizing a propagation of the periodical temperature disturbance in the sample - thermal wave methods. A few examples of thermal wave methods allowing measurement of the thermal diffusivity of bulk samples and the thermal conductivity of thin films are described. The section ends with an example of the application of thermal waves generated by sun-light for the investigation of the ground in polar regions. General conclusions on the usability of photothermal methods for determination of thermal properties, their advantages and limitations, and also possibilities for further development conclude the paper.

2. Concepts of measurement of heat transport parameters in solids

The heat transport in solids is described by the Fourier law [5]

$$\vec{j}_Q = -\kappa \vec{\nabla} T, \tag{1}$$

where $\vec{j}_Q$ is the heat flux density, T is the temperature and κ is the thermal conductivity tensor. In the case of isotropic materials or in geometries for which the heat flux density $\vec{j}_Q$ has the same direction as the temperature gradient $\vec{\nabla} T$, the thermal conductivity tensor in Eq. (1) can be substituted for the thermal conductivity κ. In this form the Fourier law is the basis of steady-flux methods for thermal conductivity measurements. As it follows from Eq. (1), to determine the thermal conductivity one has to measure the temperature gradient in the sample and the heat flux corresponding to it. The second task is not easy, and very often comparative techniques are used. There are three steady-flux standard methods for determination of the thermal conductivity of solids: the guarded-comparative-longitudinal heat flow technique [6], the heat flow meter technique [7, 8], and the guarded hot-plate technique [9, 10].

The Fourier law can not be applied for the description of non-stationary temperature fields. For this purpose the Fourier-Kirchhoff equation.

$$\rho c \frac{\partial T}{\partial t} = \vec{\nabla} \left(\kappa \vec{\nabla} T \right) + q \tag{2}$$

is used. In the last equation ρ is the mass density, c is the specific heat, and q is the density of volume heat sources. In the case of isotropic and homogeneous medium, Eq. (2) can be rewritten in the form

$$\frac{\partial T}{\partial t} = \alpha \vec{\nabla}^2 T + \frac{q}{\rho c}, \tag{3}$$

where $\alpha = \kappa / (\rho c)$ is the thermal diffusivity. Therefore in measuring techniques based on analysis of non-stationary temperature fields the thermal diffusivity is usually determined. Probably the most popular technique of this kind is the flash method. It was developed in 1961 by Parker *et al.* [11] and today it is the standard method for determination of the thermal diffusivity of solids [12, 13]. The flash method is an example of the pulse photothermal technique, where the sample to be investigated is heated by a short light pulse and the thermal diffusivity is deduced from the time evolution of the temperature field.

The thermal diffusivity can be also determined from an analysis of the propagation of periodical temperature disturbance in a sample – a thermal wave. The thermal wave arises when periodic heat sources exist in the sample [5]. In 1D model the temperature disturbance connected with the thermal wave propagating in a positive direction along the x axis is given by the equation

$$\theta = \theta_0 \exp\left(-\sqrt{\frac{\pi f}{\alpha}} x \right) \cos\left(2\pi f t - \sqrt{\frac{\pi f}{\alpha}} x + \phi_0 \right), \tag{4}$$

where θ_0 is the amplitude of the thermal wave, f is its frequency, and ϕ_0 is the initial phase. In thermal wave methods for the determination of the thermal diffusivity based upon two effects. In the simplest case the amplitude and the phase of the thermal wave are registered as functions of the distance from a source of the wave. An analysis of the amplitude decay and the phase delay allows the calculation of the thermal diffusivity. The second possibility is based upon observations of the interference of the thermal wave in a plate-form sample. Thermal waves, like other waves, reflect at boundaries of different media [14] and interfere [15]. Because of heavy damping, they do not create standing waves, nevertheless effects caused by the interference can be observed experimentally. Examples of measuring techniques based on both mentioned effects are described in the next section.

Nowadays technology widely utilizes thin films deposited on different substrates. In many cases the thermal properties of such films play a very important role and must be known. The thermal conductivity, especially in the case of dielectric materials, is strongly dependent upon internal structure. As a result the thermal conductivity of thin films can be completely different from that of the bulk material [16]. This is why methods for determination of the thermal properties of thin films are in demand. Standard photothermal techniques cannot be used for this purpose. Characteristic times measured in pulsed techniques (e.g. the flash method) are proportional to the square of the sample thickness and inversely proportional to the thermal diffusivity $\tau \propto d^2/\alpha$. For 100 nm thick film with a thermal diffusivity of 10^{-4} m^2/s, the characteristic time is of the order of 100 ps. The pulse generating the temperature disturbance should be at least 10 times shorter. So, picosecond light sources and very fast registration of temperature changes are required in the experiment. In "classical" thermal wave measurements the wavelength of the thermal wave should be comparable with the thickness of the investigated film. Using data taken for the evaluation of the characteristic time of pulse measurements one can find that the thermal wave frequency should be of the order of 100 GHz. Thermal wave experiments are practically restricted to frequencies lower than 100 MHz. Therefore, new measuring concepts are needed for characterization of thermal properties of thin films.

An interesting variant of the flash technique was proposed for the determination of the thermal diffusivity of thin metal films [17]. This method utilizes picosecond light pulses for either the generation of temperature disturbance or the observation of time evolution of the temperature field in the sample. For this reason the dependence of the reflection coefficient of the sample surface on temperature is used. The method is known as the picosecond reflectance thermometry. Its theoretical model can be found in Ref. [18].

The concept of the picosecond reflectance thermometry is quite simple, with the main drawback being the expensive equipment required. But there is also a more fundamental problem connected with investigation of very fast processes of heat transport – a proper interpretation of experimental data. As noted in the review paper [19], the concept of the temperature is based on an assumption of equilibrium within the system. The temperature is proportional to the internal energy of the system and different subsystems of it have the same temperature. During fast processes different subsystems (e.g. electrons and phonons) may not be in equilibrium and can be characterized by different temperatures. Therefore the question of applicability of the classical models to such system arises.

Another approach to the determination of the thermal properties of thin films is also possible. A film with a thickness much smaller than the wavelength of the thermal wave, deposited on a thick substrate, has practically no effect on the propagation of the thermal wave (*i.e.* does not cause considerable amplitude or phase changes). But such film changes boundary conditions. It was mentioned above that the thermal wave reflects from boundaries. So, it may also change reflection of the thermal wave at the boundary. This idea is the basis of the method for measurement of the thermal conductivity of thin films presented in the next section.

3. Selected measuring techniques

As it was mentioned in the introduction, the majority of measuring techniques described in this section utilizes mirage effect for detection of the temperature disturbance in the sample or its surrounding. The mirage effect consists in the deflection of light passing through a region with temperature gradients. Because the refractive index depends on temperature, the temperature gradients cause gradients of refractive index, and as a consequence the light beam passing through such a region deflects. The deflection signal carries information about the temperature gradients. The possibility of application of the mirage effect for signal detection in photothermal measurements was proved by Boccara *et al.* [20] and Murphy and Aamodt [21]. A probing beam passes through the region in which the thermal wave is propagating and its deflection beam gives information about the amplitude and the phase of the thermal wave. Although detailed theoretical modelling of this detection method is quite complicated [22, 23], the simplified single ray model for interpretation of experimental results is often acceptable [23].

According to this model the deflection of the probing beam is proportional to the temperature gradients integrated along the path of the probing beam. In vector notation the probing beam deflection is [24]

$$\vec{\psi} = \int_{\Gamma} \frac{1}{n}\frac{dn}{dT}\vec{\nabla}T \times d\vec{\Gamma}, \tag{5}$$

where n is the refractive index and Γ is the probing beam path. Two components of the deflection are typically considered – normal and tangential to the sample surface. This model was used for interpretation of experimental data presented in this paper.

3.1. Measurement of the thermal diffusivity of transparent materials

In the case of transparent samples the probing beam goes directly through the sample. Its deflection gives information about the temperature gradient caused by heat sources existing in the system. Two variants of experiment were used, as it is shown in Fig. 1.

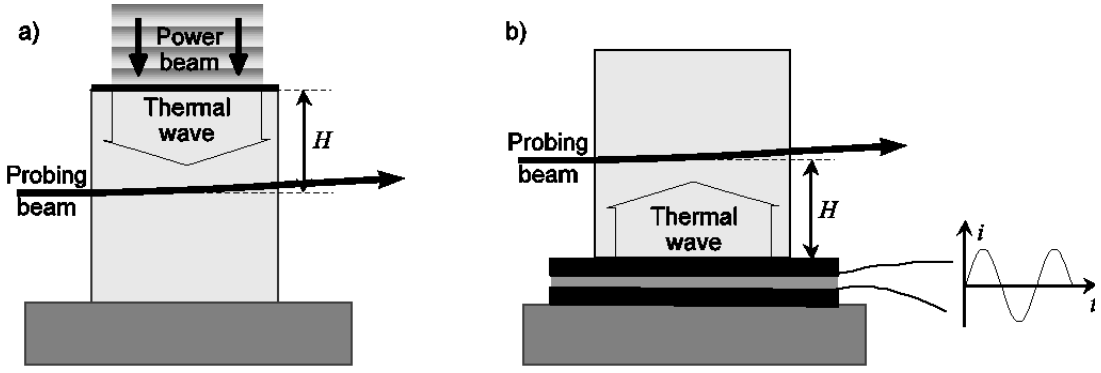

Figure 1. Variants of experiments for determination of the thermal diffusivity of bulk, transparent samples: the photothermal experiment (a), and experiment utilizing Peltier element for generation of the thermal wave (b).

They differ in the way the thermal wave is generated in the sample. In the case shown in Fig. 1a one sample wall is covered by a thin film of light absorbing material (e.g. graphite). This wall is illuminated by the intensity modulated light from a laser diode, resulting in periodical heating of the sample. In the geometry shown in Fig. 1b a Peltier element powered by alternating current is used for the same purpose. This element provides a periodical heating and cooling of one sample wall. In both cases the thermal wave generated at one wall propagates into the sample. The modulation frequency is chosen in such a way that the sample is thermally thick. This means that the sample thickness is bigger than the thermal diffusion length $(\alpha/\pi f)^{1/2}$. The thermal diffusion length is a distance at which the amplitude of the thermal wave diminishes e-times. The amplitude and the phase of the deflection signal are measured as functions of the distance from the heated wall. Because the amplitude of the signal is more sensitive to possible instability in the measuring setup than the phase, determination of the thermal diffusivity of the sample is typically based upon the analysis of the phase of the signal. Using the 1D model to describe the propagation of the thermal wave, the phase of the probing beam deflection should follow the equation

$$\phi(x) = -\sqrt{\frac{\pi f}{\alpha}}x + \phi_c, \tag{6}$$

where x is the distance from heated wall, and ϕ_c is a constant. Fitting the straight line to the dependence $\phi(x)$ one obtains the thermal diffusivity of the sample in the direction of the propagation of the thermal wave.

Exemplary results illustrating capabilities of both described variants can be found in Refs. [25–27]. The authors investigated selected single crystals used in laser technology: yttrium aluminium garnet (YAG), yttrium orthovanadate (YVO_4), lithium niobate ($LiNbO_3$), and gadolinium calcium oxoborate (GdCOB). Crystals were doped with rare-earth elements and metals. Investigated crystals have different symmetry; YAG has a cubic structure, YVO_4 belongs to the tetragonal system, $LiNbO_3$ belongs to the

trigonal system and GdCOB is the monoclinic crystal. The thermal diffusivity of cubic crystals is characterized by a single coefficient, while in the case of tetragonal and trigonal crystals two coefficients corresponding to the direction of *c* axis and the direction perpendicular to it should be determined. The thermal diffusivity of monoclinic system can be fully described by three coefficients measured for directions of axes of the optical indicatrix.

Only selected results of measurements are presented here. Dependencies obtained in investigation of Dy:$LiNbO_3$, carried out in the geometry from Fig. 1a, are shown in Fig. 2a. Results obtained in the geometry presented in Fig. 1b for GdCOB are shown in Fig. 2b. In both cases experimentally determined curves contain parts which can be fitted with a straight line as described by Eq. (6). In experiments with optical generation of the thermal wave modulation frequency did not exceed 20 Hz, while in experiments utilizing the Peltier element the upper limit of the modulation frequency was 0.4 Hz. It can be noticed that slopes of ln*A* and ϕ dependencies on *x* for the same modulation frequency are practically identical (Fig. 2a). This confirms the correctness of the theoretical model of the measurement.

It is important to note that the presented measuring techniques are fully non-destructive and are based on simple theoretical models. The accuracy of measurement is comparable with other thermal techniques.

Determined thermal diffusivities of enumerated crystals measured for different directions in the crystallographic structure and different kinds and concentration of dopants are collected in Fig. 3 and Fig. 4. Measurements revealed considerable anisotropy of the thermal diffusivity in tetragonal, trigonal and monoclinic crystals. The general rule is that dopants introduced into the crystal structure cause a decrease in the thermal diffusivity. For heavy doped crystals this decrease can even reach (30÷40)% of the value for pure crystal. Only for $LiNbO_3$ crystals lightly doped with Cu and Fe the thermal diffusivity remains practically unchanged (taking into account the measuring uncertainties). More detailed analysis of these results including consideration of possible mechanisms of the influence of dopants on the thermal diffusivity can be found elsewhere [28].

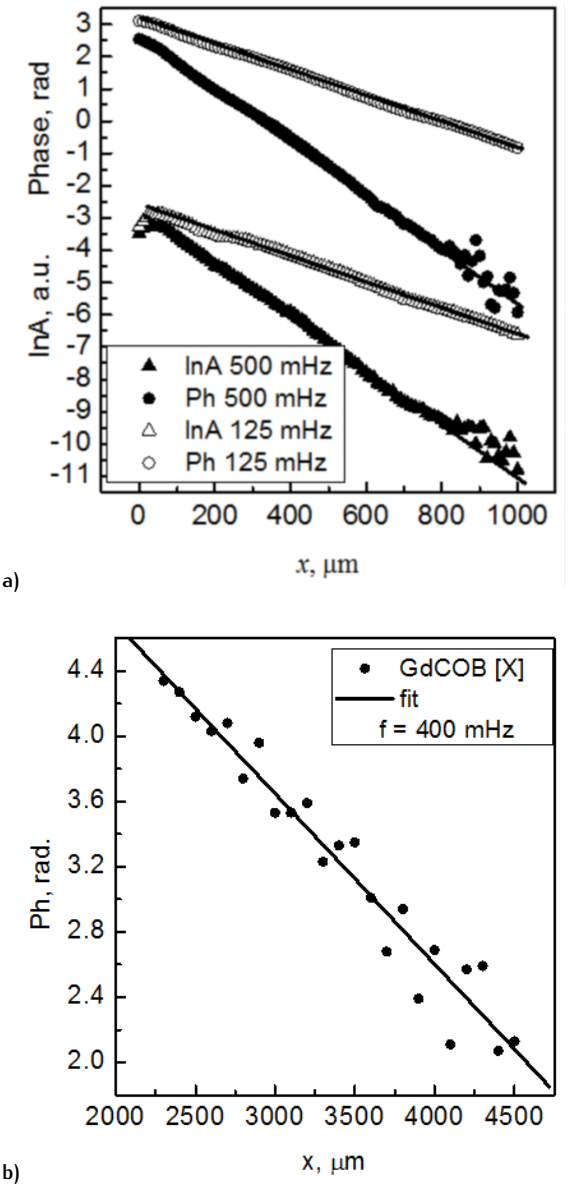

Figure 2. Exemplary experimental data obtained for: main crystallographic directions of Dy doped $LiNbO_3$ in the geometry shown in Fig. 1a at two modulation frequencies (a), and X direction of the optical indicatrix of pure gadolinium calcium oxoborate. Straight lines fitted to experimental data are also shown.

3.2. Measurement of the thermal diffusivity of plate-form samples

Measuring techniques used for the determination of the thermal diffusivity of plate-form samples can be divided into two groups. The first group comprises techniques similar to those presented in previous subsections. The geometry of measurements is shown in Fig. 5.

The thermal wave is generated at the sample surface by the intensity modulated light. It is assumed that the sample is opaque and the light is absorbed in the very thin subsurface layer. The temperature disturbance propagates through the sample and it is detected on the opposite sample surface. The problem of temperature distribution in such a configuration was analyzed elsewhere [29]. The distribution of the harmonic component of the tem-

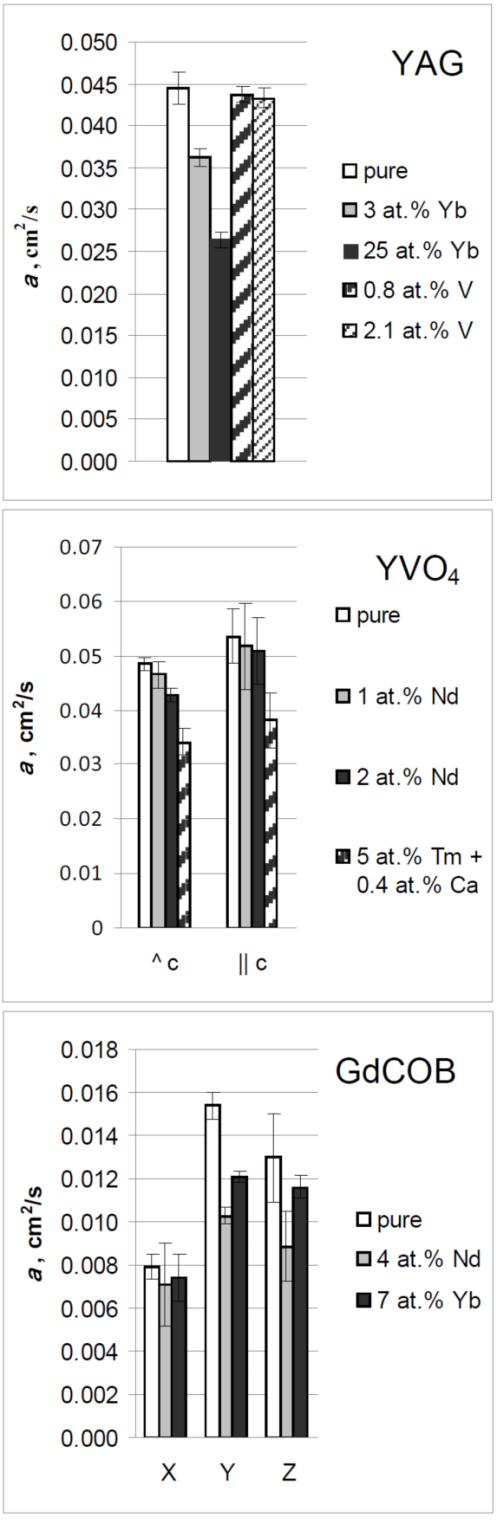

Figure 3. The thermal diffusivities of pure and doped YAG, YVO_4 and GdCOB single crystals determined in selected crystallographic directions.

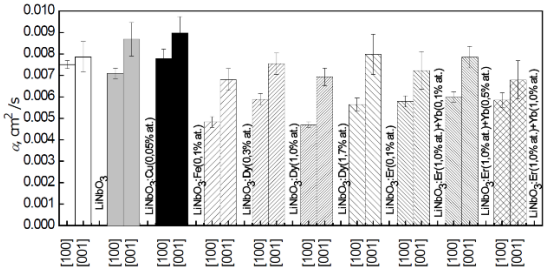

Figure 4. The thermal diffusivities of pure and doped $LiNbO_3$ single crystals in the directions perpendicular and parallel to crystallographic c axis.

perature in the sample is described by the equation

$$T(x,t) = -\frac{A}{\kappa}\sqrt{\frac{\alpha}{2i\pi f}}\,\frac{\cosh\left(\sqrt{\frac{\alpha}{2i\pi f}}\,(d-x)\right)}{\sinh\left(\sqrt{\frac{\alpha}{2i\pi f}}\,d\right)}\exp(2i\pi f t)\,, \tag{7}$$

where A is a constant related to an amplitude of the disturbance of the temperature field. It is assumed that the thermal wave propagates in the sample in the positive direction of the x axis and the power beam illuminates the plane $x = 0$. At higher frequencies, for which $\sqrt{\pi f/\alpha}\,d > 1.5$, the temperature of the plane $x = d$ can be described by the simplified formula

$$T(d,t) = -\frac{A}{\kappa}\sqrt{\frac{\alpha}{2i\pi f}}\exp\left(-i\sqrt{\frac{\pi f}{\alpha}}\,d\right)\exp(2i\pi f t)\,, \tag{8}$$

From this it is determined that the phase of the temperature disturbance at $x = d$ linearly depends on $f^{1/2}$.

Two methods of signal detection are used – photoacoustic detection (Fig. 5a) and infrared radiometry (Fig. 5b). In the first case the sample is attached to a small photoacoustic cell. Changes of sample temperature are conveyed to the gas in the cell causing periodic pressure changes, which are registered by sensitive microphones. In the second case determination of the sample temperature is based on the detection of heat radiation coming from the sample by an infrared radiation detector. The choice of the detection method in a specific experiment is connected mainly with the emissivity of the sample to be investigated. The results obtained by both techniques are practically identical. As it follows from Eq. (7) the measured signal is the function of the square root of the modulation frequency. The determination of the thermal diffusivity comes down to the fitting of a straight line to the phase dependence on $f^{1/2}$. Exemplary results obtained for copper and lead plates using different detection methods

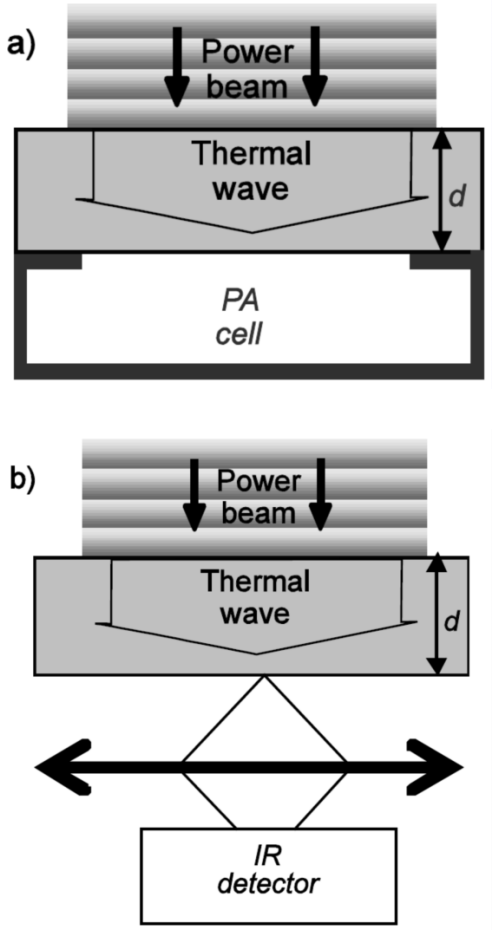

Figure 5. Variants of experiment for determination of the thermal diffusivity of opaque plate-form samples with photoacoustic (a) and IR radiometry (b) detections.

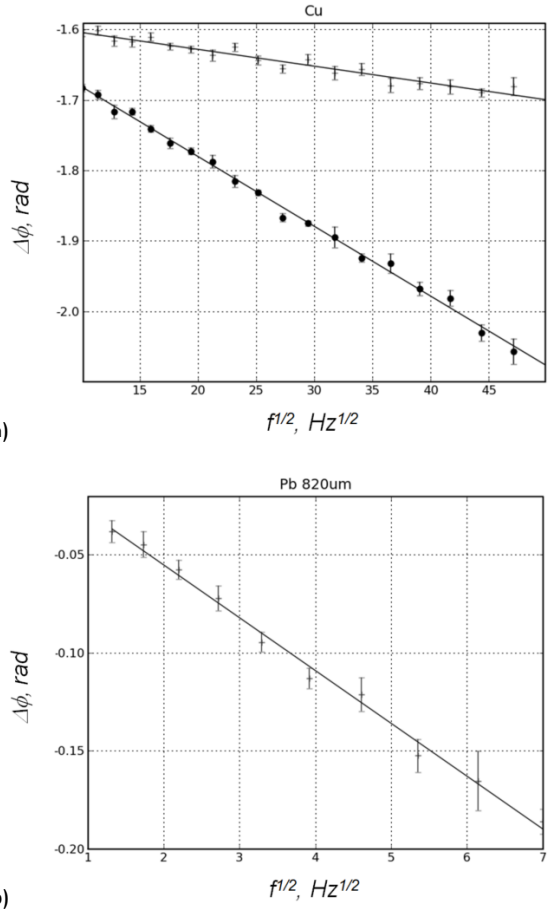

Figure 6. Exemplary dependencies of signal phase on f'' measured for two copper plates 515 μm (+) and 1020 μm (•) thick using photoacoustic detection (a) and 82 μm thick lead plate using infrared radiometry (b). Straight lines fitted to experimental points are also shown.

are shown in Fig. 6. In the case of copper experiment were carried out for 515 μm and 1015 μm thick samples. According to Eq. (8) the slope should be directly proportional to the sample thickness, which is clearly demonstrated in the respective figures below.

The thermal diffusivities obtained for selected metal plates using the described method are collected in Tab. 1. Values of the thermal diffusivity calculated from textbook data [30] are also placed for comparison. There is a very good agreement between our results and literature data.

The second group of measuring techniques allowing determination of the thermal diffusivity of samples is based upon the interference of the thermal waves in plate-form sample. These methods are described in detail elsewhere [31]. The basic idea is that the thermal wave generated at one sample surface travels to the opposite surface, reflects on it and interferes with the incidence wave. The temperature distribution in the sample is a result of this interference. In the case of the plate-like sample the temperature distribution is described by Eq. (7). In our investigations methods based on the interference of thermal waves were used mainly to determine the thermal diffusivity of semiconductor wafers. In the case of opaque samples (or samples coated with an opaque film) experiments were carried out in the geometry shown in Fig. 7a. The temperature disturbance was detected in the air above the sample as the function of $f^{1/2}$. Exemplary dependencies obtained for 520 μm thick undoped Si wafer are shown in Fig. 8a. The analysis of the signal was performed in two steps. At the beginning, basing on the high frequency part of the measured dependence, the signals were corrected for the influence of the air layer between the sample surface and the probing beam. Then theoretical curves were fitted to the amplitude and the phase of the measured sig-

Table 1. Thermal diffusivities of selected metals. For comparison, values calculated based on data on the density ρ, the specific heat c and the thermal conductivity κ from Ref. [30], and equation $\alpha = \kappa/(\rho c)$ are also placed in the table.

Metal	Meaurement	Literature [30]
Pb (99.9%)	0.246(13) cm^2/s	0.24 cm^2/s
Ti (99.7%)	0.0926(82) cm^2/s	0.093 cm^2/s
Ni (99.98%)	0.206(10) cm^2/s	0.23 cm^2/s
Cu (99.999%)	1.052(48) cm^2/s	1.16 cm^2/s
Ag (99.9%)	1.92(32) cm^2/s	1.74 cm^2/s

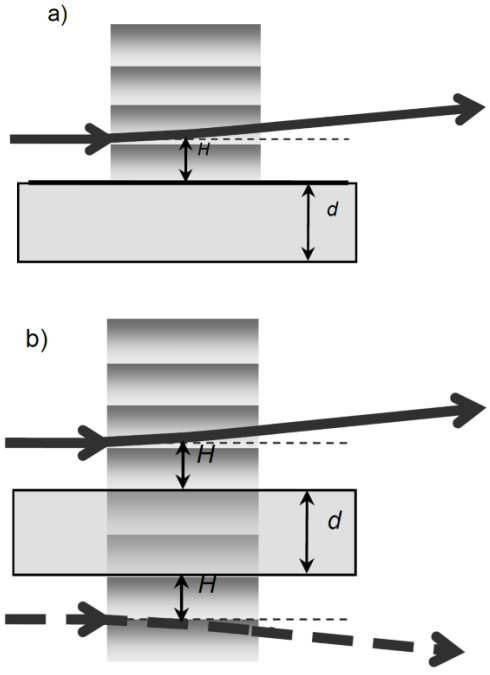

Figure 7. Variants of experiments for the thermal diffusivity measurements for opaque (a) and semi-transparent (b) plate-form samples. Both variants based on signal detection utilizing the mirage effect.

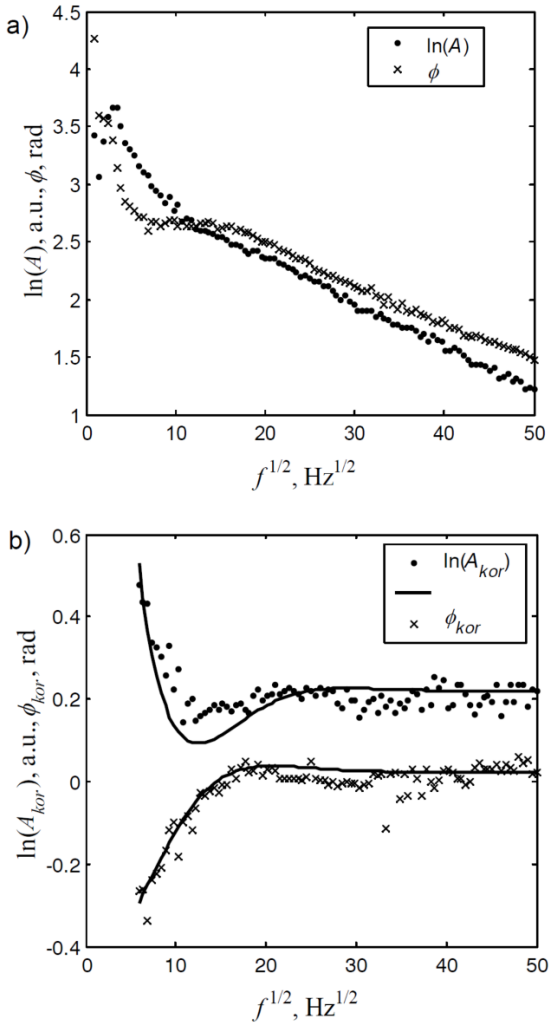

Figure 8. The amplitude and the phase of the probing beam deflection measured for 520 µm thick Si wafer in geometry shown in Fig. 7a (a), and corrected dependencies fitted with theoretical curves (b).

nal (Fig. 8b) and the thermal diffusivity of the sample was determined.

The geometry shown in Fig. 7b was used for investigation of semi-transparent wafers (e.g. SiC). Detailed descriptions of the method can be found elsewhere [32, 33]. In this paper only the basic idea of the method is presented and is illustrated by exemplary results. The difference from the previously described method consists in carrying out measurements in two configurations – for the probing beam passing over and under the sample. As in the previously described method, the amplitude A and the phase ϕ of the deflection is measured as a function of $f^{1/2}$. Then the ratio of these two signals written as complex functions of the form $A(f^{1/2})\exp[i\phi(f^{1/2})]$ was calculated and theoretical curves were fitted to the real and the imaginary parts of this ratio. Exemplary dependencies obtained for single crystal 6H SiC sample are shown in Fig. 9. This sample was a 880 µm thick plate. Because of the relatively low optical absorption of the sample the signals are quite noisy. The thermal diffusivity and the optical absorption coefficient of the sample were obtained from the multiparameter fitting procedure. Uncertainties of determined parameters were evaluated basing on the criterion of a twofold increase of a goal function from its minimum value. A few results measured for different SiC samples are collected in Tab. 2.

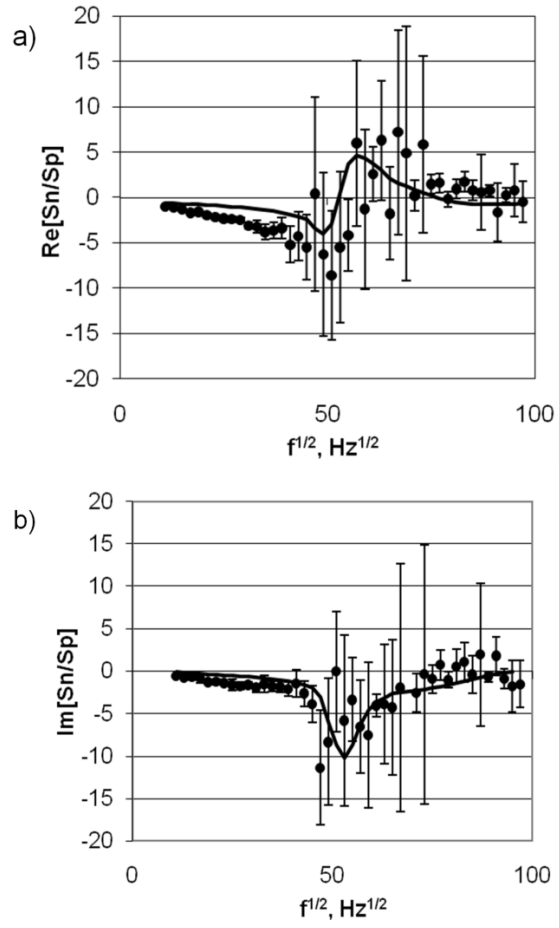

Figure 9. The real and the imaginary part of the ratio of signals measured in the geometry shown in Fig. 7b for single crystal of 6H SiC. Fitted theoretical curves are also shown.

The samples can be divided into two groups: polycrystalline wafers (samples #1 - #3) and single crystals (samples #4 and #5). The samples #1 and #2 were cut from the same wafer but contain different concentrations of structural defects. Sample #3 was produced by another manufacturer. It can be seen that defected sample has considerably lower thermal diffusivity. Supplementary investigation revealed that sample #3 has also higher optical absorption than samples #1 and #2. So, the differences in the thermal properties of investigated samples are probably caused by different grain structures and concentration of structural defects. Values obtained for single crystal samples are much higher than those for polycrystalline wafers. The uncertainty of these measurements is about 10%. A more detailed description of the method can be found elsewhere [33].

Table 2. The thermal diffusivity α and the optical absorption γ of SiC wafers with different crystalline structure. The uncertainty of determined thermal diffusivities is about 10%, while the uncertainty on the optical absorption is about 25%. All polycrystalline samples had thicknesses of about 500 µm, while the single crystal samples were about 900 µm thick.

Sample	Description	α [cm^2/s]	γ [cm^{-1}]
#1	poly-SiC (4H), manufacurer #1, high quality	0.51	24
#2	poly-SiC (4H), manufacurer #1, with defects	0.24	18
#3	poly-SiC (4H), manufacurer #2	0.22	70
#4	SiC (6H)	1.4	18
#5	SiC (6H)	1.15	13

3.3. Investigation of the thermal properties of thin films

As it was stated in Section 2, determination of the thermal properties of the thin film deposited on the thick substrate is a complex measuring problem. The main reason is that the effective thermal properties of thin film – substrate system is practically not affected by the thin film. Let us consider a thin film of the thickness d and the thermal conductivity κ_f deposited on a substrate of the thickness L and the thermal conductivity κ_s. The effective thermal conductivity of such a system can be written as

$$\kappa_{eff} = \kappa_f \kappa_s \frac{d+L}{\kappa_f L + \kappa_s d}. \tag{9}$$

In the case of typical electronic structures $L \sim 500$ µm and $d \sim 0.1$ µm, therefore $\kappa_{eff} \approx \kappa_s$. This means that it is necessary to look for measuring techniques in which the influence of the thin film on experimental dependencies will be more pronounced. Two methods presented in this subsection based on the influence of the thin film on boundary conditions at the sample – surrounding interface. The film can be treated as a thermal resistance $R_{th} = d/\kappa_f$ at the substrate-surrounding boundary. In both cases the thermal conductivity of the thin film is deduced from the comparison of signals measured in two geometries chosen in such a way that in one of them the influence of the thin film on the measured signal is negligible.

The first method utilizes a 1D model of thermal wave propagation in the layered structure. Details of the method can

be found in Ref. [34] - only a basic idea of this method is presented here. Measurements were carried out in the two geometries shown in Fig. 10. To determine the thermal conductivity of the thin film the ratio of measured dependencies of the deflection signals on $f^{1/2}$ for both geometries were calculated. Then, the amplitude and the phase of this ratio were fitted with theoretical curves. Exemplary results for two diamond-like carbon films deposited on Si wafers are shown in Fig. 11. The films differ in thickness. The estimated thermal conductivity is 2.6 $Wm^{-1}K^{-1}$ for the 1.32 µm thick film, and 2.5 $Wm^{-1}K^{-1}$ for the 0.65 µm thick film. The ratios of the photothermal signals are quite noisy, thus the measuring uncertainty is relatively high and averages about 25%. So, values obtained for both layers are practically the same.

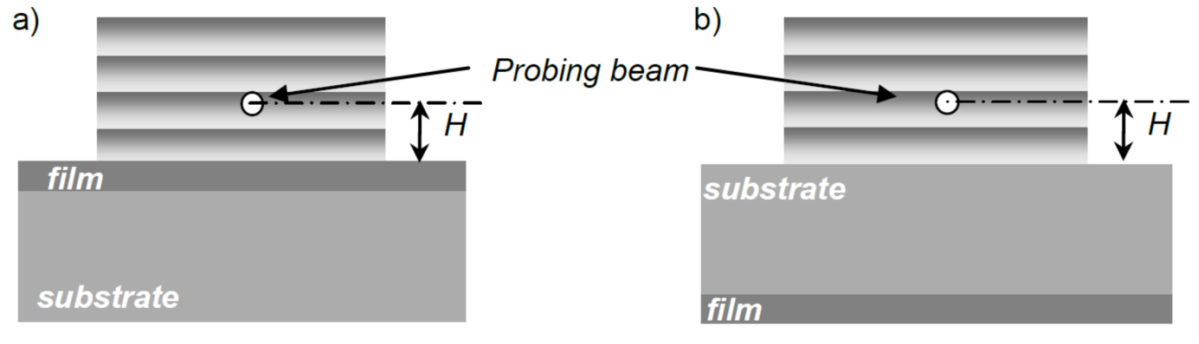

Figure 10. Experimental geometries of investigation of the thermal conductivity of thin films based on 1D propagation of the thermal wave: front illumination a), rear illumination b).

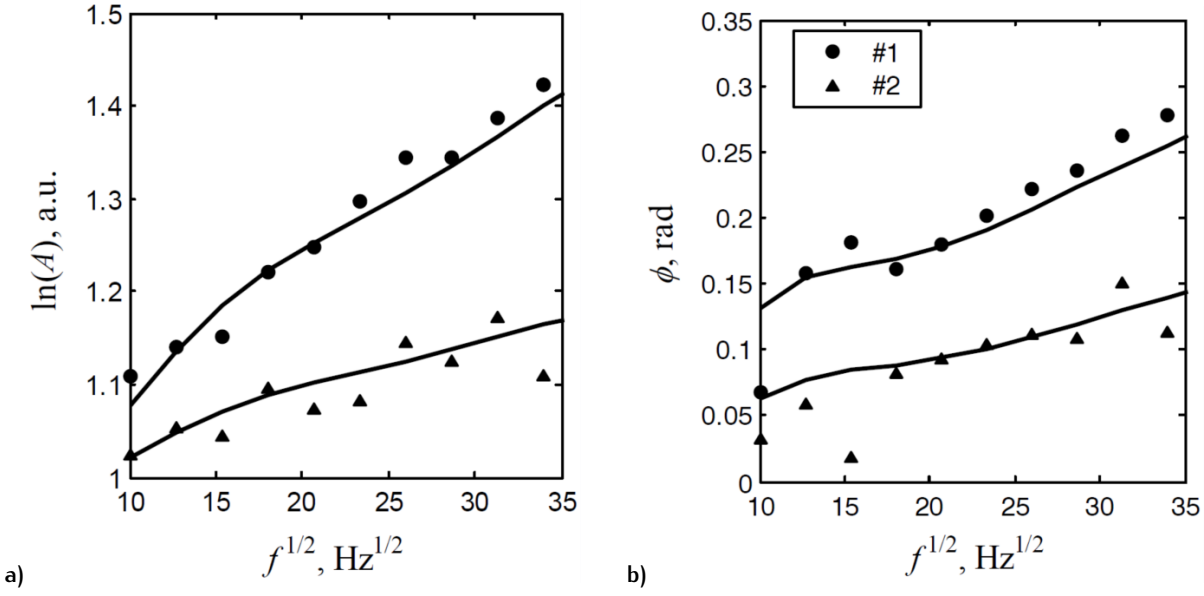

Figure 11. The amplitudes and the phases of the ratios of signals measured in geometries shown in Fig. 10 for two diamond-like carbon films deposited on Si. The film thicknesses were: 1.32 µm (#1) and 0.65 µm (#2).

The second technique, described in detail in Ref. [35], is based on a very similar idea but the thermal wave is generated by tightly focused light beam and the 3D model of the thermal wave propagation is used. Experiments are also carried out in two configurations (Fig. 12). However in this case the normal and the tangential components of the deflection of the probing beam are registered as functions of the distance between the axes of the generating and the probing beams. Unfortunately it is not possible to use analytical formulas for the measured signals in normal space. This is the reason for the transformation of measured dependencies into the inverse space (wave-vector space). In the wave-vector space the measured signal can be described analytically and the analysis of experimental data is simpler.

The ratios of transformed signals, for both the normal and the tangential components, are calculated and then the phase of these ratios is fitted with theoretical curves. It is important in this procedure that the ratios of the transformed signals calculated for the normal and the tangential deflection components should be the same. This fact can be used as a criterion for the correctness of measurement. Exemplary results obtained by described method for 200 nm thick HfO_2 film deposited on 340 μm thick Si substrate are shown in Fig. 13. It is clearly seen that dependencies obtained for normal and tangential deflections are almost the same. The thermal conductivity of the thin film is estimated from the fitting of the theoretical curve to the dependence calculated from experimental data. The uncertainty of this measurement is about 15%

Thermal conductivities determined by this method for different thin films are collected in Tab. 3. Three types of thin films were investigated. The AlN and AlN+GaN films were used as passivating and antireflective coatings in semiconductor lasers. Investigated films were deposited on different substrates. Their effective thermal conductivities are 2 to 3 orders of magnitude lower than thermal conductivities of respective bulk materials. It was also possible to determine the thermal conductivity of films thicker than 100 nm. The same concerns the ZnO film, which can be used as transparent electric contact. HfO_2 films reveal higher thermal conductivity. Investigated HfO_2 films were deposited at different concentrations of O_2. The highest thermal conductivity has the film obtained at the lowest O_2 concentration (10%), while the lowest thermal conductivity was found in the film obtained at 20% O_2 concentration. There is no simple dependence between the oxygen concentration and the thermal conductivity of the thin film. To explain experimentally obtained results the topography of HfO_2 films was additionally investigated using an atomic force microscope (AFM). The topography images are shown in Fig. 14. Root-mean-squared roughness calculated for presented data is 1.50 nm for the 10% O_2 sample, 0.96 nm for the 20% O_2 sample and 1.19 nm for the 30% O_2 sample. Lower roughness means that the layer is built of smaller grains. So, the HfO_2 film obtained at 10% of O_2 consists of the biggest grains and it has the highest thermal conductivity, whereas the film obtained at 20% of O_2 has the smallest grains and therefore has the lowest thermal conductivity.

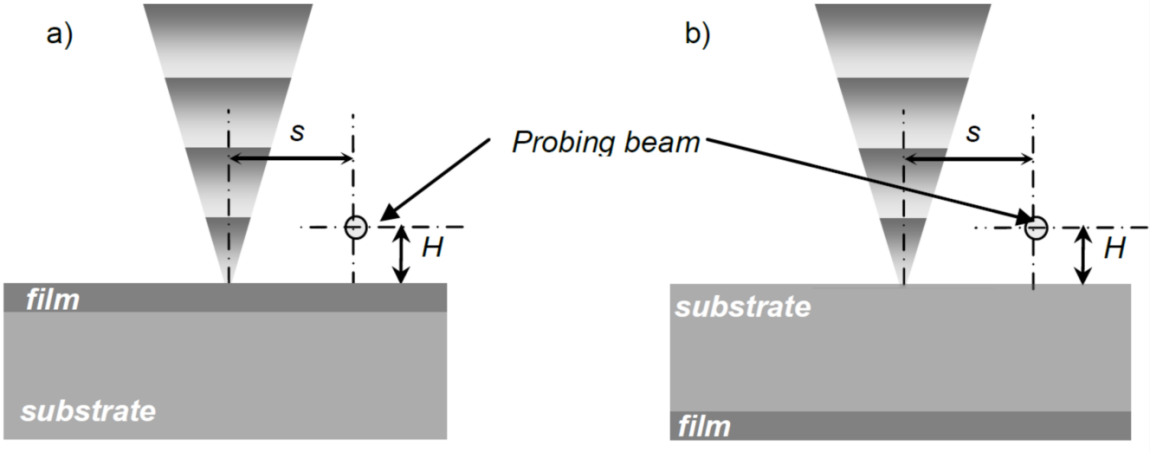

Figure 12. Experimental geometries of investigation of the thermal conductivity of thin films based on 3D propagation of the thermal wave: front illumination a), rear illumination b).

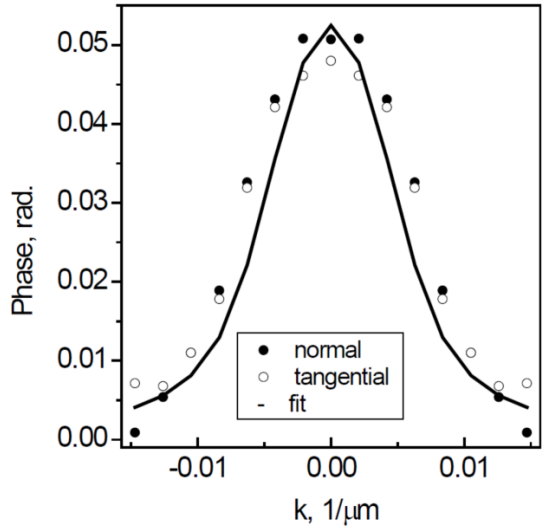

Figure 13. The ratio of signals measured in geometries shown in Fig. 12 and transformed to the inverse space with fitted theoretical curve. The measurement was carried out for 200 nm thick HfO_2 films deposited on nSi at 10% O_2 concentration.

Table 3. Thermal conductivity of thin dielectric films determined from photothermal experiments.

Thin film (d [μm])	Substrate (L [μm])	κ [W/(m K)]
GaN+AlN (0.220 + 0.030)	Si (490)	0.070
GaN+AlN (0.220 + 0.030)	GaAs (410)	0.230
AlN (0.270)	Si (490)	0.014
AlN (0.270)	GaAs (410)	0.042
ZnO (0.375)	GaSb:Te (470)	0.160
HfO_2 (10% O_2) (0.200)	Si (340)	4.96
HfO_2 (20% O_2) (0.200)	Si (340)	1.89
HfO_2 (30% O_2) (0.200)	Si (340)	3.23

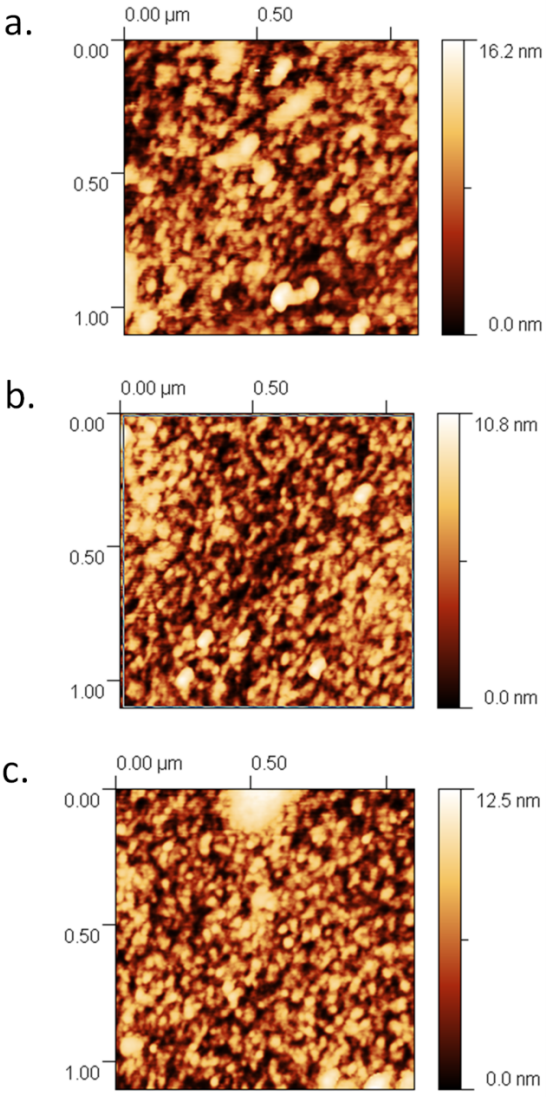

Figure 14. AFM topographic images of 200 nm thick HfO_2 films obtained at 10% (a.), 20% (b.) and 30% (c.) O_2 concentrations.

3.4. Investigation of the ground in a polar region

Thermal wave methods can be used not only at the laboratory scale. The results presented in this subsection confirm the applicability of these methods for investigation of much bigger objects. As an example the analysis of thermal waves generated in the ground by sun-light is shown. Processes of freezing and thawing of the ground in polar regions are widely investigated by geophysicists. Information about temperatures at different depths are collected over long time periods and analyzed. Measurements presented here were carried out in a tundra near the Polish Polar Station (Hornsund, SW Spitsbergen)[1]. The data collected during the polar summer reveals propagation of the thermal wave in the ground (Fig. 15).

From the phase shifts of this thermal wave at different depths the thermal diffusivity of consecutive ground layers can be estimated. It is shown that the thermal diffusivi-

[1] *The measuring setup used for these experiments was developed and built by one of the authors of this paper (JM) The equipment was placed in selected locations by Piotr Dolnicki during his stay in the polar station.*

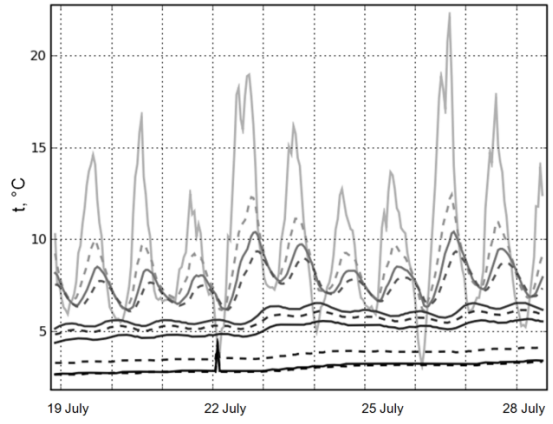

Figure 15. Thermal waves generated in the ground by sun-light in the polar region. Presented curves correspond to different depths as follows: 0.5 cm, 10 cm, 20 cm, 30 cm, 40 cm, 50 cm, 60 cm, 80 cm, and 100 cm. The bigger depth, the lower mean temperature and the daily oscillations.

ties of ground layers are related to their composition and humidity (year period). Some preliminary results of this analysis are shown in Tab. 4. The uncertainty of thermal diffusivity evaluation is about 25%. More details about possibilities of use of thermal wave methods in the investigation of active permafrost layers can be found elsewhere [36].

4. Conclusions

Examples of different thermal wave methods presented in this paper confirm their usefulness in investigation of thermal properties of various materials and structures. The majority of these methods, similarly to other non-stationary thermal measurements, leads to determination of the thermal diffusivity with an uncertainty of about 10%. As opposed to standard technical methods which require samples with dimensions of a few centimeters, methods described in this paper allow the measurement of thermal diffusivity of much smaller samples, e.g. 0.5 mm thick substrates, which are common in semiconductor technology. It is important to note that using intensity modulated light to induce temperature disturbance and infrared radiometry or mirage effect for signal detection fully non-contact measurement can be realized. In spite of simplified theoretical models of measurement the methods presented here permit examination of anisotropic samples, even single crystals of relatively low symmetry. In this case properly oriented and cut samples are required.

Table 4. Thermal diffusivity of ground layers in tundra in selected months.

Month	Depth: from 0 to 20 cm Material: gravel and small stones	Depth: from 20 cm to 40 cm Material: gravel and sand	Depth: bigger than 40 cm Material: gravel, sand, clay and rocks
Jun.	8.3×10^{-3} cm^2/s	6.9×10^{-3} cm^2/s	34×10^{-3} cm^2/s
Aug.	14.2×10^{-3} cm^2/s	11.6×10^{-3} cm^2/s	28×10^{-3} cm^2/s
Sep.	12.1×10^{-3} cm^2/s	–	–

In the typical thermal wave techniques, similarly to other wave methods, the wavelength should not be longer than sample dimensions (layer thickness). It is very difficult, and often impossible, to fulfill this requirement in the case of thin, submicron films. The problem can be partially solved by analysis of the influence of a film on the boundary conditions at a sample-surrounding interface instead of analysis of the thermal wave propagation in the film Presented results confirm the usefulness of such measurements for determination of the thermal conductivity of dielectric films thicker than 100 nm.

Thermal wave measurements can be realized using reasonably standard laboratory equipment. It is shown that using a medium-power laser diode or a Peltier element to generate the thermal wave and a low-power HeNe laser for the detection of the temperature disturbance, a wide range of samples can be investigated. In peculiar cases naturally arisen thermal waves can be also utilized The accuracy of the thermal wave measurement is typically about 10 to 15% and is comparable with the accuracy of other thermal techniques.

In general the theoretical description of the propagation of the temperature disturbance in inhomogeneous medium is a rather complicated problem Nevertheless a simple 1D model can very often be used for interpretation of experimental data. As long as the diameter of the source of

the thermal waves (heated area) is a few times bigger than the thermal wave length, the 1D approximation gives satisfactory results.

As it is stated above thermal wave measuring methods are suitable for investigation of films not thinner than about 100 nm. The investigation of thermal properties of smaller objects remain an unsolved problem. New possibilities in this field are given by a short pulse lasers (the picosecond reflectance thermometry mentioned in the section 2) and scanning thermal microscopy

References

[1] C. Kittel, Introduction to solid state physics (John Wiley and Sons, New York, Chichester, 1996)
[2] P. K. Schelling, L. Shi, K. E. Goodson, Mater. Today 6, 30 (2005)
[3] U. Schulz et al., Ceram. Eng. Sci. Proc. 25, 375 (2004)
[4] J. Bodzenta, Thermal waves in investigations of solids (Silesian University of Technology, Gliwice, Poland, 1999)
[5] H. S. Carslaw, J. C. Jaeger, Conduction of heat in solids (Oxford Science Publications, New York, 1986)
[6] ASTM E1225-04: Standard Test Method for Thermal Conductivity of Solids by Means of the Guarded-Comparative-Longitudinal Heat Flow Technique
[7] ASTM C518-04: Standard Test Method for Steady-State Thermal Transmission Properties by Means of the Heat Flow Meter Apparatus
[8] ASTM E1530-04:Standard Test Method for Evaluating the Resistance to Thermal Transmission of Materials by the Guarded Heat Flow Meter Technique
[9] ASTM C177–04: Standard Test Method for Steady-State Heat Flux Measurements and Thermal Transmission Properties by Means of the Guarded-Hot-Plate Apparatus
[10] ISO 8302:1991 Thermal insulation – Determination of steady-state thermal resistance and related properties – Guarded hot plate apparatus
[11] W. J. Parker, R. J. Jenkins, C. P. Butler, G. L. Abbott, J. Appl. Phys. 32, 1679 (1961)
[12] ASTM E1461-07: Standard Test Method for Thermal Diffusivity by the Flash Method
[13] ISO 18755:2005 Fine ceramics (advanced ceramics, advanced technical ceramics) - Determination of thermal diffusivity of monolithic ceramics by laser flash method
[14] D. Y. Tzou, Int. J. Heat Mass Tran. 36, 401 (1993)
[15] A. Mandelis, K. F. Leung, J. Opt. Soc. Am. A 8, 186 (1991)
[16] J. Bodzenta, Chaos, Solitons and Fractals 10, 2087 (1999)
[17] C. A. Paddock, G. L. Eesley, J. Appl. Phys. 60, 285 (1986)
[18] D. G. Cahill, Rev. Sci. Instrum. 75, 5119 (2004)
[19] D. G. Cahill, K. Goodson, A. Majumdar, J. Heat Transf. 124, 223 (2002)
[20] A. C. Boccara, D. Fournier, J. Badoz, Appl. Phys. Lett. 36, 130 (1980)
[21] J. C. Murphy, L. C. Aamodt, J. Appl. Phys. 51, 4580 (1980)
[22] A. L. Glazov, K. L. Muratikov, Tech. Phys.+ 38, 344 (1993)
[23] D. Korte Kobylińska, R. J. Bukowski, B. Burak, J. Bodzenta, S. Kochowski, J. Appl. Phys. 100, 063501 (2006)
[24] L. C. Aamodt, J. C. Murphy, J. Appl. Phys. 52, 4903 (1981)
[25] J. Bodzenta, W. Hofman, M. Gała, T. Łukasiewicz, M. Pyka, J. Phys. IV 129, 195 (2005)
[26] J. Bodzenta, M. Pyka, J. Phys. IV 137, 259 (2006)
[27] J. Bodzenta, A. Kaźmierczak-Bałata, T. Łukasiewicz, M. Pyka, Eur. Phys. J.Spec. Top. 153, 135 (2008)
[28] J. Bodzenta, A. Kaźmierczak-Bałata, K. Wokulska, J. Kucytowski, T. Łukasiewicz, W. Hofman, Appl. Optics 48, C46 (2009)
[29] J. Bodzenta et al., Dent. Mater. 22, 617 (2006)
[30] D. R. Lide, CRC Handbook of Chemistry and Physics, 84th edition (CRC Press, Boca Raton, Florida, 2008)
[31] J. Bodzenta, J. Mazur, R. Bukowski, Z. Kleszczewski, Proc. SPIE 2643, 286 (1995)
[32] J. Bodzenta, A. Kaźmierczak-Bałata, J. Phys. IV 137, 245 (2006)
[33] J. Bodzenta et al., Eur. Phys. J.-Spec. Top. 153, 79 (2008)
[34] J. Bodzenta, J. Mazur, Z. Kleszczewski, Journal of Chemical Vapor Deposition 5, 288 (1997)
[35] J. Bodzenta, B. Burak, A. Jagoda, B. Stańczyk, Diam. Relat. Mater. 14, 1169 (2005)
[36] J. Mazur, P. Dolnicki, J. Phys. IV 109, 59 (2003)